Application of the Theory of Martensite Crystallography to Displacive Phase Transformations in Substitutional Nonferrous Alloys

B.C. MUDDLE, J.F. NIE, and G.R. HUGO

It has been demonstrated that the theory of martensite crystallography is capable of accounting successfully for the form and crystallography of a range of plate- or lath-shaped transformation products, even when the formation of the product phase involves significant substitutional diffusion. These transformations include the precipitation of metastable hexagonal γ' (Ag_2Al) plates in disordered face-centered cubic (fcc) solid-solution Al-Ag alloys, the formation of ordered AuCu II plates from disordered fcc solid solution in equiatomic Au-Cu alloys, and the formation of metastable $9R$ α_1 plates in ordered ($B2$) Cu-Zn and Ag-Cd alloys. The application of the theory to these transformations is reviewed critically and the features common to them identified. It is confirmed that, in all three transformations, the product phase produces relief at a free surface consistent with an invariant plane-strain shape change and that the transformations are thus properly described as displacive. The agreement between experimental observations and theoretical predictions of the transformation crystallography is in all cases excellent. It is proposed that successful application of the theory implies a growth mechanism in which the coherent or semicoherent, planar interface between parent and product phases maintains its structural identity during migration and that growth proceeds atom by atom in a manner consistent with the maintenance of a correspondence of lattice sites. In the case of the coherent, planar interfaces associated with γ' precipitate plates in Al-Ag alloys, there is direct experimental evidence that this is accomplished by the motion of transformation dislocations across the coherent broad faces of the precipitate plates; the transformation dislocations define steps that are two atom layers in height normal to the habit plane and have a Burgers vector at least approximately equivalent to an $(a/6)\langle 1\bar{1}2\rangle$ Shockley partial dislocation in the parent fcc structure. However, for AuCu II plates, where the product phase is twinned on a fine scale, and for α_1 plates, for which the lattice invariant strain leads to a substructure of finely spaced stacking faults, the structures of the semicoherent interphase boundaries and thus the details of the transformation mechanism remain less clearly defined.

I. INTRODUCTION

IN the approximately 40 years since the original formulations[1,2] of the crystallographic theory of martensitic transformations first appeared, the theory[3] has been applied successfully to classically diffusionless martensitic transformations in a wide range of metallic[4,5,6] and ceramic systems.[7] The theory has not yet proved to be of universal applicability to such transformations. However, the large number of transformations to which it has been shown to be applicable, and the accuracy with which it has proved capable of accounting for the crystallographic features of these transformations, have led to general acceptance of the theory as providing a reliable basis for predicting transformation crystallography. During that same period, the theory has also been applied to a number of transformations for which the transformation product exhibits morphology and crystallography typical of a martensitic product, but which involve significant long-range diffusion or atomic interchange over distances exceeding unit cell dimensions. These transformations include the formation of Widmanstätten[8] and bainitic ferrite[9–12] in steels, and the precipitation of a range of hydride,[13,14] nitride,[15] and oxide[16,17] products, where it is conveniently assumed that the displacive component of the transformation involves the substitutional constituents alone and that the compositional change accompanying transformation is accomplished by essentially independent interstitial diffusion.

However, there are also members of this class of transformations which involve a composition change or ordering reaction that inevitably requires vacancy diffusion and for which it is thus more difficult to reconcile the displacive and diffusional components of transformation. It is the purpose of the present article to review the applicability of the formal crystallographic theory to selected transformations in this latter category and to examine critically the implications of successful application of the theory for the mechanism of transformation.

B.C. MUDDLE, Reader in Materials Engineering, is with the Department of Materials Engineering, Monash University, Clayton, Victoria, 3168 Australia. J.F. NIE, formerly with the Department of Materials Engineering, Monash University, is Research Fellow with the Department of Mining and Metallurgical Engineering, University of Queensland, St. Lucia, Queensland, 4072 Australia. G.R. HUGO, formerly with the Department of Materials Engineering, Monash University, is Research Scientist with Aeronautical Research Laboratory, Defence Science and Technology Organisation, Fishermens Bend, Victoria, 3207 Australia.

This article is based on a presentation made at the Pacific Rim Conference on the "Roles of Shear and Diffusion in the Formation of Plate-Shaped Transformation Products," held December 18–22, 1992, in Kona, Hawaii, under the auspices of ASM INTERNATIONAL's Phase Transformations Committee.

The three transformations examined are those that have attracted by far the most attention and controversy: the face-centered cubic (fcc) to hexagonal close-packed (hcp) transformation associated with the precipitation of metastable γ' phase in Al-Ag alloys,[18–23] the formation of ordered orthorhombic CuAu II plates from disordered fcc solid solution in equiatomic Cu-Au,[24–30] and the *B*2 to 9*R* transformation associated with the formation of metastable α_1 plates in Cu-Zn(-X)[31–39] and Ag-Cd alloys.[40,41]

II. CRYSTALLOGRAPHIC THEORY

The initial step in the application of the crystallographic theory to any transformation involves the identification of the correspondence between parent and product lattices that is characteristic of martensitic transformations and which relates uniquely vectors, planes, and unit cells of the parent with corresponding vectors, planes, and cells in the product phase. It is the maintenance of this lattice correspondence that allows the change in structure to be described by a homogeneous lattice deformation, **B**. When combined with an appropriate rigid body rotation, **R**, this homogeneous strain defines a total lattice strain, $\mathbf{S_T} = \mathbf{R} \cdot \mathbf{B}$, that generates the product lattice in its observed orientation relationship with the parent phase. For a given transformation, it is commonly assumed[42] that the operative lattice correspondence will be that which involves the minimum principal deformations (η_i) for the strain **B**, and this correspondence may often be identified simply by inspection of the crystal structures of parent and product phases and the observed orientation relationship between them. The homogeneous strain **B** is completely defined by the assumed lattice correspondence and the lattice parameters of parent and product lattices.

The total lattice strain $\mathbf{S_T}$ is rarely such that it leaves a plane of the parent structure undistorted and unrotated in the product, and, for most transformations, it is incompatible with a plate-shaped transformation product with an invariant habit plane and a macroscopic shape deformation that is an invariant plane strain. This discrepancy is resolved by considering the shape strain $\mathbf{S_R}$ to be the product of the total lattice strain $\mathbf{S_T}$ and a second strain **L**, which is lattice invariant and which occurs inhomogeneously throughout the transformed volume so as to maintain an interface plane that is macroscopically undistorted, *i.e.*, $\mathbf{S_R} = \mathbf{S_T} \cdot \mathbf{L}$. In the simplest form of the theory, the lattice invariant strain **L** is assumed to be the product of slip or a partial twinning shear in parent or product lattices. Alternatively, the total lattice strain $\mathbf{S_T}$ may be represented as the product of consecutive invariant plane strains, *i.e.*, $\mathbf{S_T} = \mathbf{S_R} \cdot \mathbf{L}^{-1}$, and is thus an invariant line strain, with the invariant line parallel to the line of intersection of the habit plane and the plane of lattice invariant shear (LIS). Given as input the lattice correspondence and lattice parameters of initial and final lattices, and the plane and direction of LIS, the theory permits calculation of the magnitude, plane, and direction of the shape strain $\mathbf{S_R}$, the magnitude of the LIS, and the predicted orientation relationship between lattices.

Solutions to the theory can exist only if the homogeneous lattice deformation **B** is such that at least one of the principal deformations is less than unity and one greater than unity. If, in addition, the remaining principal deformation is exactly unity, then $\mathbf{S_T}$ is itself an invariant plane strain and there is no requirement for an LIS. In such a transformation, the two lattices related by **B** may be fully coherent across a planar interface. The classic example of such a transformation is the fcc (f) to hcp (h) transition occurring in pure Co,[43] certain Co-based alloys,[44,45,46] and a range of highly alloyed steels of relatively low stacking fault energy.[6,47] In this case, the interatomic spacings within parallel close-packed planes are very nearly identical in the fcc and hcp structures, and the change in structure may be simply accomplished by a shear, equivalent to one-half the twinning shear, between alternate pairs of $\{111\}_f$ planes in any one of the three $\langle 112 \rangle_f$ twinning directions in a given $\{111\}_f$ plane.[48] The magnitude of this shear is $(8^{-1/2})$* and, if the shear occurs on a single shear system, then the shear component of the shape deformation is appreciable (~0.35). If, however, shear occurs in all three $\langle 112 \rangle_f$ directions in a given $\{111\}_f$ habit plane, then the transformation may be partially or wholly self-accommodating and the shear component of the shape strain may vary from a maximum of $8^{-1/2}$ to zero. In the latter extreme, the shape deformation $\mathbf{S_R}$ may be considered to be the average of equal volumes of the three possible lattice deformations such that $\mathbf{S_R} = \mathbf{I}$, where **I** is the identity matrix.[49]

The glissile motion of a rational, coherent interface as an entity is energetically unfavorable, and it is commonly assumed that transformations for which the interface is fully coherent proceed *via* the formation and migration of transformation dislocations across the otherwise planar interface (Figure 1). The transformation dislocations constitute atomic scale steps on the interface and, following Christian,[48,49,50] have an effective Burgers vector of

$$\mathbf{b_T} = hm\mathbf{d} = h\tau\mathbf{t} + h\xi\mathbf{n} \qquad [1]$$

where h is the step height, m is the magnitude of the shape strain, **d** is a unit vector defining the direction of the shape strain, **t** is a unit vector in the direction of the shear component of the strain, **n** is a unit vector normal to the habit plane, and τ and ξ are the magnitudes of the shear and normal components of displacement, respectively. In general, the Burgers vector is not a lattice vector in either parent or product lattices. In the specific case of the fcc to hcp transformation, the minimum step height corresponds to the spacing of two close-packed planes normal to the coherent interface plane, and a transformation dislocation that will accomplish the required structural adjustment in the packing of the close-packed planes has the following Burgers vector:[49]

$$\mathbf{b_T} = \frac{a}{6}\langle 112 \rangle + \frac{2\xi a}{3}\langle 111 \rangle \qquad [2]$$

---

*This value is based on the assumption that the two structures are perfectly coherent in the habit plane and that the hcp structure has the ideal axial ratio of $(8/3)^{1/2}$.

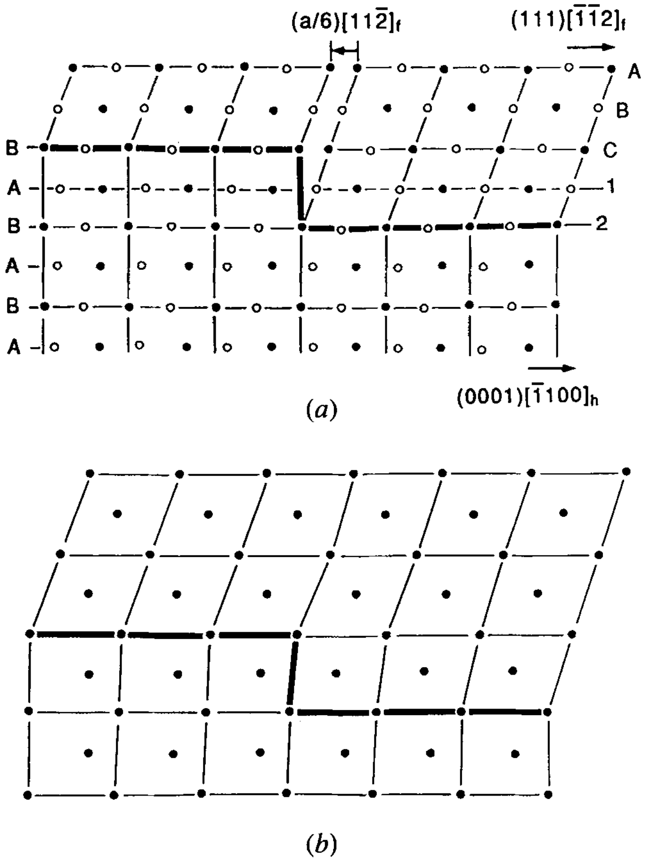

Fig. 1—(*a*) The $(111)_f \| (0001)_h$ interface between fcc and hcp structures containing a step that is two atom layers in height normal to the interface. Open and filled circles represent atoms on successive planes of the type $(2\bar{2}0)_f$ or $(11\bar{2}0)_h$. Note that planes 1 and 2 are common to both structures. (*b*) Schematic representation of the resulting transformation dislocation with Burgers vector $(a/6)[11\bar{2}]$.

This transformation dislocation reduces to a simple Shockley partial dislocation of the fcc structure if there is no change in the spacing of the close-packed planes normal to the habit plane (*i.e.*, $\xi = 0$). In the schematic representation of the fcc to hcp transition shown in Figure 1, the transformation dislocation has the specific Burgers vector $(a/6)[11\bar{2}]$.

In those transformations for which the total lattice strain $\mathbf{S_T}$ does not itself allow a plane between parent and product lattices to remain invariant, the crystallographic theory allows for the total strain to be combined with a lattice invariant strain **L** to define a habit plane which is macroscopically invariant and across which there is sufficient structural continuity to permit rapid glissile motion of the interface. Two simple models of a semicoherent martensitic interface, compatible with the formal requirements of the theory, have emerged.[5,48] In the first, the LIS is assumed to involve slip in either parent or product lattices, and the misfit in the interphase boundary is accommodated discontinuously by a single array of parallel interface dislocations with a common Burgers vector and a spacing determined by the magnitude of the LIS required to preserve a planar interface. The dislocation lines lie parallel to the intersection of the LIS plane and the habit plane, and are thus parallel to the invariant line **l** of $\mathbf{S_T}$. The interface is glissile and may move readily as an entity normal to itself, provided that the individual dislocations may move conservatively with the interface on slip planes in parent and product lattices that meet edge-on in the interface. This will be the case provided that the Burgers vector of the dislocations is either not parallel to the interface or, in the case of pure screw dislocations, is parallel to the invariant line **l**.

In the second of the models of a semicoherent martensitic interface, the mismatch at the interface is corrected periodically by what is normally fine-scale twinning of the product phase, and the LIS corresponds to a partial twinning shear of the product lattice. In this case, the accommodation within the habit plane extends over the widths of individual twins, and the theory determines the relative widths of the twin-related crystals required to achieve a habit plane that is macroscopically invariant. If the fractions of the two twin orientations are f_t and $(1 - f_t)$, then there are two solutions for the equivalent lattice invariant shear with magnitudes:

$$g_1 = f_t s \quad \text{and} \quad g_2 = (1 - f_t)s \qquad [3]$$

where s is the magnitude of the twinning shear on the appropriate system in the product lattice. In the simplest form of this model, the segments of interface between each of the twin orientations and the parent phase are assumed to be in a state of forced elastic coherence and the interface is dislocation-free.[50] The elastic strain field associated with the interface has a periodicity equivalent to the average combined width of adjacent twin pairs, which is to be compared with the spacing of the interface dislocations in the dislocation model discussed previously. The interface is readily glissile, and growth of the product phase is assumed to involve motion of the interface as an entity normal to itself.

These models of coherent and semicoherent martensitic interfaces are such as to permit a correspondence of lattice sites to be preserved between parent and product lattices, and, provided that this correspondence is not destroyed by simultaneous diffusion, they imply a shape change over the transformed volume that may be described by an invariant plane strain. The assumption of a lattice correspondence is intrinsic to the application of formal crystallographic theory, and successful application of the theory, together with the observation of an invariant plane-strain shape change, would seem to imply the maintenance of a lattice correspondence. It is to be emphasized that, being phenomenological in nature, the theory requires a correspondence of equivalent lattice sites and not necessarily the maintenance of a correspondence of atoms occupying equivalent positions. It has been commonly assumed, however, that any significant atomic interchange over distances typically larger than the dimensions of the unit cell would destroy the correspondence of lattice sites and any associated shape change.[51] This argument is usually justified on thermodynamic grounds; the additional strain energy that would necessarily accompany a change of shape is considered likely to provide a driving force for the elimination of the correspondence under conditions permitting rapid atomic interchange.[51] A potential exception to this proposal has been identified in those cases, such as the formation of Widmanstätten or bainitic ferrite, where a change in composition is achieved through diffusion of a highly mobile interstitial constituent, while the displacive component of the transformation is sustained by a constituent for which the range of atom movements remain less than the scale of the unit cell. However, it has long been considered unlikely that a shape change would be sustained and that the crystallographic theory would be proved applicable for those transformations that involve significant long-range substitutional (*i.e.*, vacancy) diffusion. The transformations reviewed here appear to constitute notable exceptions to this expectation and thus continue to attract significant attention.

III. PRECIPITATION OF γ' PHASE IN Al-Ag ALLOYS

A. *Experimental Observations*

In Al-Ag alloys containing typically 15 to 20 wt pct Ag, solution-treated (550 °C, 0.5 hour), quenched, and aged (350 °C to 400 °C, 0.5 hour), the supersaturation of Ag in fcc solid solution is relieved initially by the precipitation of a metastable γ' phase and eventually by formation of the equilibrium γ (Ag_2Al) precipitate phase. The transition from γ' to γ phase occurs directly within individual precipitate particles and is described[19] as being associated with a loss of coherency of the γ' particles. The coherent γ' and semicoherent γ phases are both hcp, differ by only small changes in lattice parameters,[19,22] and are thus difficult to distinguish by most conventional diffraction techniques. However, most of the very extensive and detailed experimental work that has been carried out on the system[18–23] has been concerned with the initial stages of precipitation. The present discussion will thus focus on the formation of the γ' phase.

The crystal structure that has been proposed[23] for the γ' phase is, as shown in Figure 2, hcp ($a = 0.2858$ nm, $c = 0.4607$ nm, $c/a = 1.612$), with alternating close-packed A and B layers of pure Ag and Al_2Ag, respectively, to give an average precipitate composition of Ag_2Al. Although yet to be confirmed, this structure is qualitatively consistent with detailed contrast analysis of high-resolution images of γ' plates, and electron diffraction evidence confirms that the phase exhibits long-range order on alternate basal planes during at least the initial stages of growth. The γ' phase precipitates as thin, hexagonal-shaped plates with large aspect ratios (10:1 to 100:1) on $\{111\}_\alpha$ planes of the α-Al matrix ($a_o = 0.4059$ nm). The orientation relationship between parent and product structures is such that $(0001)_\gamma \| (111)_\alpha$ and $[11\bar{2}0]_\gamma \| [1\bar{1}0]_\alpha$. The two lattices are almost perfectly coherent within the $(0001)_\gamma \| (111)_\alpha$ habit plane, and there is a difference of only ~1.7 pct[23] in the spacing of the close-packed planes normal to the habit plane.

The transformation associated with the formation of γ' plates is thus structurally similar to the martensitic fcc to hcp transformation in Co and Co-based alloys.[43–46,48–50] However, there can be no question that there is a substantial composition change involving long-range substitutional diffusion of Ag associated with the formation of the γ' plates. Plates of the γ' phase have, for example, been extracted from the α-Al matrix and analyzed using energy-dispersive X-ray spectroscopy, and the composition has been confirmed to be consistent with the compound Ag_2Al to within ~4 at. pct.[23] Despite this composition change, there is ample evidence that there may be a shape change associated with the formation of γ' and γ plates, and that those plates formed at a free surface produce a surface relief consistent with a shape deformation that is an invariant plane strain.[19,21] Measurements of the surface tilt for single plates have been reported to be consistent with a simple shear equivalent to one-half of the twinning shear (0.354) in the hcp lattice.[21]

B. *Application of the Theory*

The structural change from fcc to hcp associated with the precipitation of the γ' phase is readily interpreted in terms of the formal crystallographic theory.[48,49,50] Based on the lattice parameters discussed previously, the misfit in interatomic spacings along parallel close-packed directions within the common close-packed planes is <0.5 pct. If it is assumed that the structures are perfectly coherent in the habit plane at the transformation temperature, and that there is no change in the spacing of the close-packed planes normal to the habit plane, then the structural change may be considered to be accomplished by a simple shear of magnitude $8^{-1/2}$ on the $(111)_f$ plane in the $[11\bar{2}]_f$ direction. In the formalism of the theory, the total strain $\mathbf{S_T}$ is an invariant plane strain equivalent in this case to the shape deformation $\mathbf{S_R}$:

$$\mathbf{S_T} = \mathbf{S_R} = \mathbf{I} + m\mathbf{d}\mathbf{p}' \qquad [4]$$

where $\mathbf{I}$ is the identity matrix, m is the strain magnitude, $\mathbf{d}$ is a unit vector in the direction of displacement, and $\mathbf{p}'$ is a unit vector normal to the shear plane. Using a three-axis system to define the basis of the hcp lattice, the lattice correspondence between hcp and fcc lattices compatible with the observed orientation relationship is, as shown in Figure 3, of the form

$${}_{\mathrm{f}}\mathbf{C}_{\mathrm{h}} = \frac{1}{2}\begin{bmatrix} 0 & 1 & 1 \\ \bar{1} & 0 & 1 \\ 1 & \bar{1} & 2 \end{bmatrix} \quad \text{and} \quad {}_{\mathrm{h}}\mathbf{C}_{\mathrm{f}} = \frac{1}{2}\begin{bmatrix} 1 & \bar{3} & 1 \\ 3 & \bar{1} & \bar{1} \\ 1 & 1 & 1 \end{bmatrix} \qquad [5]$$

The total strain may be expressed[48] as

$$\mathbf{S_T} = \frac{1}{12}\begin{bmatrix} 13 & 1 & 1 \\ 1 & 13 & 1 \\ \bar{2} & \bar{2} & 10 \end{bmatrix} \qquad [6]$$

For the present transformation, the lattice parameters imply a reduction of ~1.7 pct in the spacing of the close-packed planes parallel to the habit plane, and the displacement vector $m\mathbf{d}$ thus has a component normal to the habit plane. From Eq. [2],

$$m\mathbf{d} = \mathbf{b_T} = \frac{a}{6}[11\bar{2}] - \frac{2 \times 0.017a}{3}[111] \qquad [7]$$

and the total lattice strain

$$\mathbf{S_T} = \begin{bmatrix} 1.0364 & 0.0364 & 0.0364 \\ 0.0364 & 1.0364 & 0.0364 \\ -0.0808 & -0.0808 & 0.9192 \end{bmatrix} \qquad [8]$$

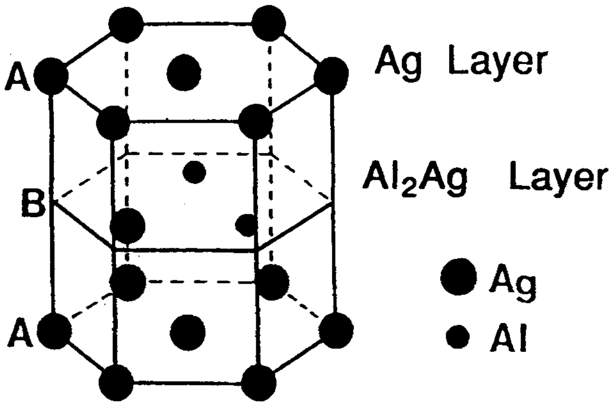

Fig. 2—Schematic representation of the crystal structure proposed for the γ phase (Ag_2Al) in Al-Ag alloys.[23]

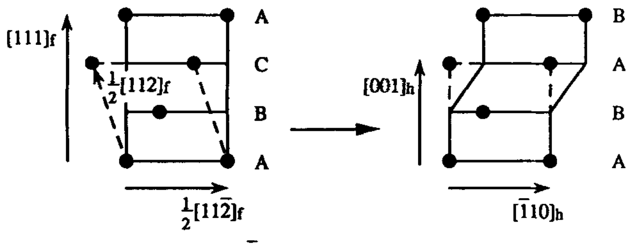

Fig. 3—Schematic representation of the lattice correspondence between parent and product lattices for the fcc to hcp transformation.

is an invariant plane strain rather than a simple shear. This total lattice strain S_T defines phenomenologically both the change in structure and the shape deformation.

IV. FORMATION OF ORDERED AuCu II PLATES IN EQUIATOMIC Au-Cu

A. *Experimental Observations*

Equiatomic Au-Cu has a disordered fcc structure (a_c = 0.3872 nm) at temperatures above 410 °C and is ordered below this temperature. Below 380 °C, the product of ordering (AuCu I) is face-centered tetragonal (fct) $L1_0$ (a_t = 0.395 nm, c_t = 0.368 nm, c/a = 0.932),[25] with alternate layers of Au and Cu atoms parallel to the (001) basal plane. In the interval between 380 °C and 410 °C, a one-dimensional long-period superlattice designated AuCu II is formed. The orthorhombic unit cell of the AuCu II corresponds to an assembly of ten $L1_0$ unit cells stacked parallel to [010], with antiphase domain boundaries every five unit cells characterized by a displacement vector of the form ${}^1/_2[101](010)$. Each $L1_0$ cell suffers a small additional distortion parallel to [010], and it has become common to describe the AuCu II structure in terms of the resulting orthorhombic (o) pseudocell with a_o = 0.3979 nm, b_o = 0.3963 nm, and c_o = 0.3678 nm.[25]

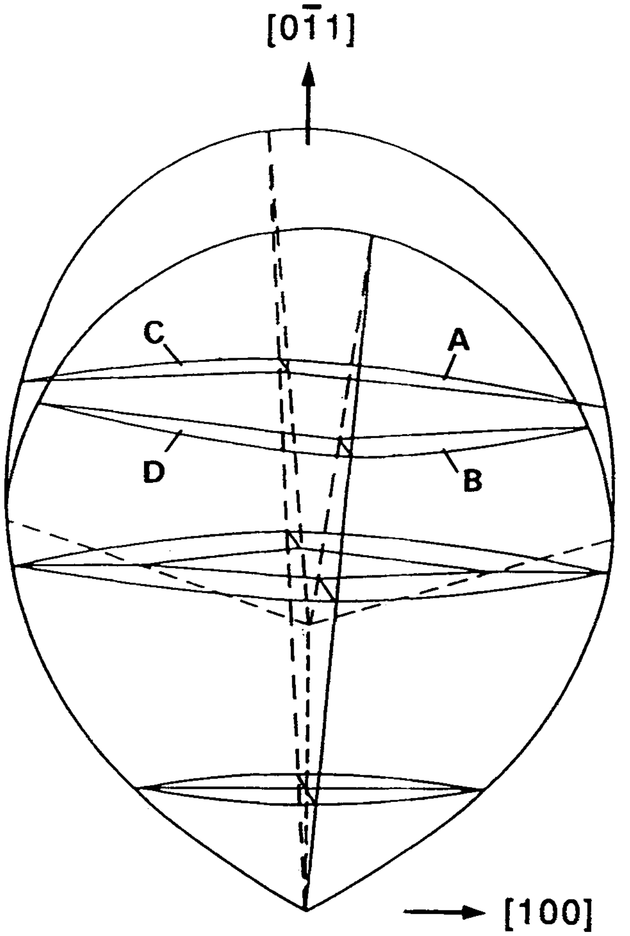

Fig. 4—Schematic representation of the morphology of AuCu II plates forming a pyramidal group of four.[29]

The ordered AuCu II phase forms characteristically as plates in pairs or pyramidal groups of four which, as shown schematically in Figure 4, share a common apex and grow cooperatively by motion of the inner apex parallel to the $[0\bar{1}1]$ axis of the pyramid.[29] The forms that the plates are observed to take in section depends on the location and orientation of the plane of section with respect to the pyramid axis. The range of forms consistent with the pyramid morphology proposed in Figure 4 are shown in the reflected-light micrograph of Figure 5(a). At a free surface, the plates produce a well-defined surface relief (Figure 5(b)), which has been shown[25] to be consistent with an invariant plane-strain shape deformation. The inner and outer surfaces of the AuCu II plates are not parallel, leading to some uncertainty in the determination of the true habit plane. However, it is well established that the habit plane is irrational and close to {011}. Within a pyramidal group of four plates, the habit plane poles cluster close to a single $(0\bar{1}1)$ plane, as shown schematically in Figure 4. The results of habit plane measurements from one such group, determined from trace measurements in two surfaces,[25] are reproduced in Figure 6, where it is clear that they are equivalent variants of a single irrational plane to within ±1 deg.

The orientation relationship between ordered AuCu II and disordered cubic (c) matrix is such that the principal axes of the ordered phase are approximately parallel to those of the matrix.[25,52] This is illustrated using electron diffraction in Figure 7, where the AuCu II plate in

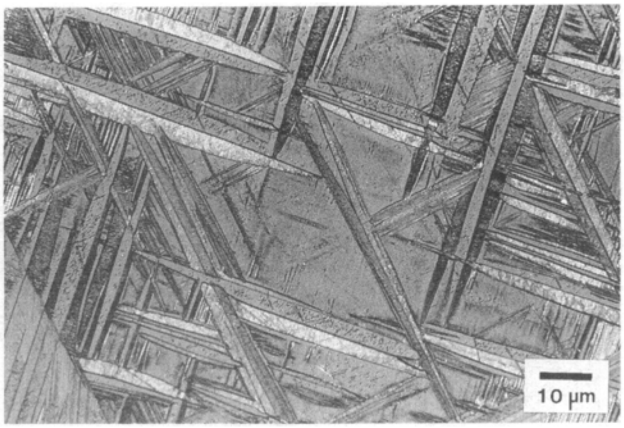

(*a*)

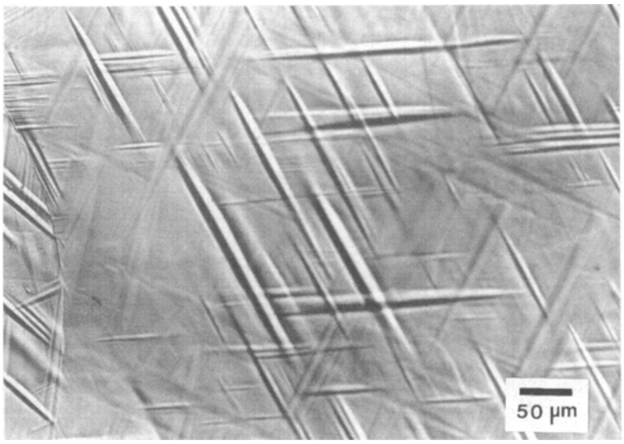

(*b*)

Fig. 5—Reflected light micrographs of (*a*) polished and etched section showing AuCu II plates in an equiatomic Au-Cu alloy aged 0.75 h at 390 °C;[52] and (*b*) surface relief on a prepolished surface associated with growth of AuCu II plates produced under similar conditions.[52]

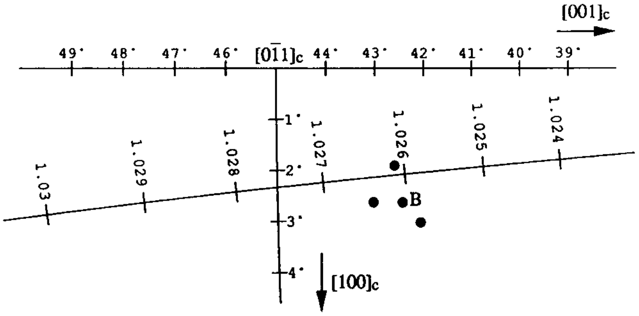

Fig. 6—Stereographic projection comparing the positions of measured habit plane normals for a pyramidal group of four AuCu II plates[29] with the locus of predicted habit planes plotted as a function of lattice parameter ratio a_o/a_c, where a_c refers to the fcc matrix and a_o refers to the orthorhombic product, for fixed values of the ratios b_o/a_o = 0.9960 and c_o/a_o = 0.9244. The measured habit planes have been converted by symmetry operations to that variant B consistent with the assumed variant of the LIS, *i.e.*, (101)[$\bar{1}$01]$_o$. Measured lattice parameters[25] give a_o/a_c = 1.0276.

Figure 7(a) is oriented with a $\langle 001 \rangle_o$ direction parallel to the incident electron beam.[52] The accompanying selected-area electron diffraction (SAED) pattern (Figure 7(b)) includes reflections from the cubic matrix and from two $[001]_o$ variants of the ordered orthorhombic structure, twin-related about a $\{101\}_o$ plane. For the indexing adopted in Figure 7(c), the measured deviation of the $(001)_o$ plane from $(001)_c$ is on the order of 2 deg, and that between (100) planes is also approximately 2 deg. More accurate measurements of the angles between principal axes determined in previous work[25] using X-ray diffraction are reproduced in Figure 8 for a plate with habit plane variant equivalent to variant B in Figures 4 and 6.

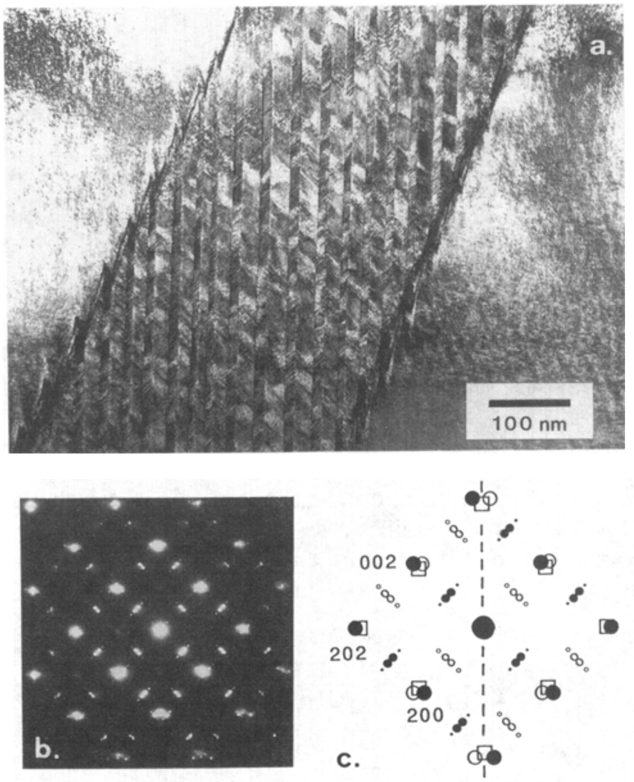

Fig. 7—(*a*) Transmission electron micrograph of single AuCu II plate recorded with the electron beam parallel to a ⟨100⟩ fcc matrix direction; (*b*) corresponding SAED pattern; and (*c*) schematic indexed solution to (b) showing two $[010]_o$ variants of the orthorhombic product phase (open and filled circles) twin-related about $(101)_o$. Those reflections represented by open squares define an $[010]_c$ zone of the matrix phase.[52]

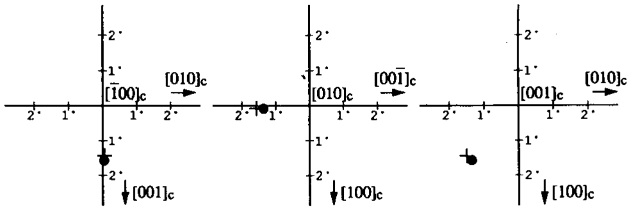

Fig. 8—Local sections of stereographic projections comparing measured[25] (crosses) and calculated (closed circles) positions of the principal axes of the orthorhombic unit cell of AuCu II plotted with respect to the principal axes of the parent fcc lattice. The variant of the orientation relationship shown corresponds to the variant B of the habit plane in Fig. 6.

As indicated in Figure 7, the AuCu II plates have a substructure of fine-scale twins on a $\{101\}_o$ twin plane. The pair of AuCu II plates shown in Figure 9 were imaged with the electron beam parallel to $\langle 111\rangle_c$ matrix and to corresponding $\langle 111\rangle_o$ axes in each of the plates. In this orientation, the twin planes in both plates and the junction plane between plates are parallel to the electron beam, and the habit planes of both plates are also approximately edge-on. Electron microdiffraction patterns recorded from the plates have been used to confirm[52] that each comprises twin-related variants of the ordered structure and that the variant that is in the lesser fraction is common to each. If the plates are interpreted, as indicated, as an A,B pair (*c.f.* Figure 4) and the electron beam is assumed to be parallel to $[\bar{1}11]_c$, then the twin plane for plate B is $(101)_o$ and the trace normal to the habit plane is observed to deviate by approximately 3 deg from $(0\bar{1}1)_o$ toward $(101)_o$. These electron microscope observations are thus consistent with earlier results,[25] which established that the twin plane corresponding to the habit plane variant B was $(101)_o$, derived from the corresponding $(101)_c$ plane of the parent phase.

When the $\{101\}_o$ twin plane is oriented parallel to the electron beam, as in Figure 9, it is possible to make accurate measurements of the relative thicknesses, x_1 and x_2, of the two twin-related orientations in the AuCu II plates. The results of measurements[52] of the average twin widths for a series of six different plates imaged under these conditions are recorded in Table I. Each value of twin width represents an average of at least 15 individual measurements on a given plate. The twin width ratio, x_2/x_1, has an average value of 0.49 ± 0.05.

B. *Application of the Theory*

The crystallographic theory has been applied[25] to the formation of AuCu II plates assuming that the correspondence between parent and product lattices is identity and that the LIS comprises a partial twinning shear on the system $\{101\}_o\langle\bar{1}01\rangle_o$. The predictions of the theory, for the specific variant of the correspondence

$$ {}_oC_c = \begin{bmatrix} 1 & 0 & 0 \\ 0 & 1 & 0 \\ 0 & 0 & 1 \end{bmatrix} \qquad [9] $$

and an LIS on the system $(101)[\bar{1}01]$, are presented in Table II. These predictions vary with a variation in the input lattice parameters, and a segment of the locus of predicted habit planes as a function of lattice parameter ratio for the low shear solution (2A) is shown in Figure 6. The curve passes close to $(0\bar{1}1)$ and, for the measured lattice parameter ratio of 1.0276, the predicted habit plane is within 3 deg of the measured habit plane variant B, for which the twin plane variant has been confirmed experimentally to be $(101)_o$ (Figure 9). In the original application of the theory, this difference between measured and predicted habit planes was interpreted[25] in terms of a dilatation parameter δ, which was considered a component of the shape strain and in essence relaxed the condition that the habit plane remains completely undistorted by allowing a small uniform dilatation of the habit plane. However, there is little or no direct evidence to support such a dilatation in this or other such transformations, and it appears likely that this difference is attributable to the difficulty of identifying the true habit plane for the tapered plates and to experimental errors in measurement.

For the previous low shear solution, the predicted shape strain direction is approximately parallel to $[011]_f$ and the magnitude of the shape deformation is ~0.047. Although there have been no direct measurements of the shape strain to date, the predicted shape strain has been used to calculate the surface tilts expected for CuAu II plates in certain orientations, and both the sense and magnitudes of these tilts have been found to be in excellent agreement with experimental observations.[25]

Aside from providing accurate predictions of the components of the shape strain consistent with the observed crystallographic variants, it is also to be emphasized that, by considering appropriate variants of the lattice correspondence and the LIS, the theory permits four variants of the low shear solution, for which the habit plane poles cluster about $(0\bar{1}1)_f$, in the manner observed experimentally. The theory is thus capable of accounting for the crystallography of each pyramidal group of four plates, for which the shape strain directions cluster about $[011]_f$. Each group of four may be considered to comprise two pairs in which the shear components of the shape strain are largely self-accommodating to minimize the net shape deformation.

As indicated in Table II, the principal axes of the product phase are predicted to be close to parallel to those of the cubic parent phase and, as shown in Figure 8, the agreement between the predicted and measured[25] orientation relationship for variant B is excellent. The twinned substructure of the AuCu II plates implies an LIS whose magnitude is determined by the relative proportions of the twin-related orientations within the plates. The magnitude g of the LIS has been

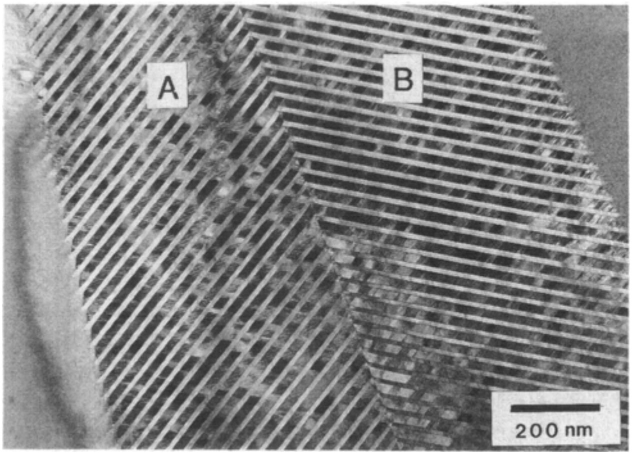

Fig. 9—Transmission electron micrograph showing a pair of AuCu II plates recorded with the electron beam parallel to a $\langle 111\rangle_c$ axis and to corresponding $\langle 111\rangle_o$ axes in each of the plates. The twin planes in both plates and the junction plane between plates are parallel to the electron beam, and the habit planes of both plates are also approximately edge-on.

Table I. Measurements of the Relative Twin Widths and the Magnitude (g) of Lattice Invariant Shear in AuCu II Plates[52]

Plate	x_1 (nm)	x_2 (nm)	x_2/x_1	g
1	12.71	6.32	0.497	0.052
2	21.32	11.32	0.531	0.055
3	30.87	13.64	0.442	0.048
4	21.83	10.87	0.498	0.052
5	21.13	11.37	0.538	0.055
6	24.25	10.73	0.442	0.048
Average:			0.49 ± 0.05	0.052 ± 0.005

Table II. Predictions of the Crystallographic Theory for the Disordered fcc to Ordered Orthorhombic Transformation Associated with the Formation of AuCu II Plates

Lattice Parameters: $a_c = 0.3872$ nm
$a_0 = 0.3979$ nm, $b_0 = 0.3963$ nm, $c_0 = 0.3678$ nm
Lattice Invariant Shear System: $(101)_0[\bar{1}01]_0$
Lattice Correspondence: Identity

					Orientation Relationship: Direction Cosines of Product Axes		
Solution	g*	Habit Plane Normal Direction Cosines	Shape Strain Direction Cosines	m**	a_0	b_0	c_0
1A	0.1024	0.7044, −0.7087, 0.04104	−0.7209, −0.6918, −0.04200	0.04736	0.9984	0.02364	0.05121
					−0.02364	0.9997	−0.002587
					−0.05126	0.001377	0.9987
1B	0.1024	0.7044, 0.7087, 0.04104	−0.7209, 0.6918, −0.04200	0.04736	0.9984	−0.02364	0.05121
					0.02354	0.9997	0.002587
					−0.05126	−0.001377	0.9987
2A	0.0546	0.04104, −0.7087, 0.7044	−0.04200, −0.6918, −0.7209	0.04736	0.9996	0.001377	0.02730
					−0.000731	0.9997	−0.02367
					−0.02732	0.02364	0.9994
2B	0.0546	0.04104, 0.7087, 0.7044	−0.04200, 0.6918, −0.7209	0.04736	0.9996	−0.001377	0.02730
					−0.000731	0.9997	0.02367
					−0.02732	−0.02364	0.9994

*g is the magnitude of the lattice invariant strain.
**m is the magnitude of the shape strain.

calculated[52] from the measured twin widths x_1 and x_2 reported in Table I using the following expression:

$$g = \left(\frac{x_2}{x_1 + x_2}\right)s = f_2 s \qquad [10]$$

where s is the magnitude of the twinning shear and f_2 represents the volume fraction of orientation 2 in the orthorhombic product. For these lattice parameters, the magnitude of the twinning shear,[5] $s = [(a/c + c/a)^2 - 4]^{1/2}$ is 0.1575 and the resulting magnitudes of g in Table I vary between 0.048 and 0.055 for the six plates examined.[52] The average value for g over the six plates is 0.052 ± 0.005 and is thus in excellent agreement with the predicted value of 0.055 shown in Table II.

V. FORMATION OF α_1 PLATES IN Cu-Zn(-X) AND Ag-Cd ALLOYS

A. *Experimental Observations*

When body-centered cubic (bcc) β-phase alloys, based on the systems Cu-Al, Cu-Sn, Cu-Zn, and Ag-Cd, are quenched from temperatures at which the β phase is stable, there is invariably an ordering transition to a CsCl-type ($B2$) structure (β'). The β' phase is metastable and, on cooling below room temperature, undergoes martensitic transformation to one or more transformation products. In Cu-Zn alloys, two forms of martensite have been reported, one which inherits the ordered CuAu I structure (fct) from the matrix β' phase and has a substructure of fine-scale twinning, and a second needlelike martensite that has a faulted substructure and the $9R$ crystal structure, which may be regarded as a variant of the conventional close-packed fcc (f) structure ($3R$) with an $(a/6)\langle 112\rangle$ $\{111\}$ displacement on every third close-packed plane. However, if the β' phase in Cu-Zn alloys containing typically 38 to 44 wt pct Zn is reheated to temperatures in the two-phase ($\alpha + \beta'$) field, isothermal decomposition occurs and, at the lower end of the transformation temperature range, a metastable plate-shaped product designated α_1 is formed. The α_1 plates produce a surface relief consistent with an invariant plane-strain shape deformation[31,32,36] and have a morphology, structure, and crystallography closely similar to that of the needlelike $9R$ martensite formed athermally at low temperatures.[53,54]

Figure 10(a) shows the results of habit plane measurements for α_1 plates formed isothermally in two Cu-Zn alloys[36] and a Ag-Cd alloy,[40] plotted with respect to

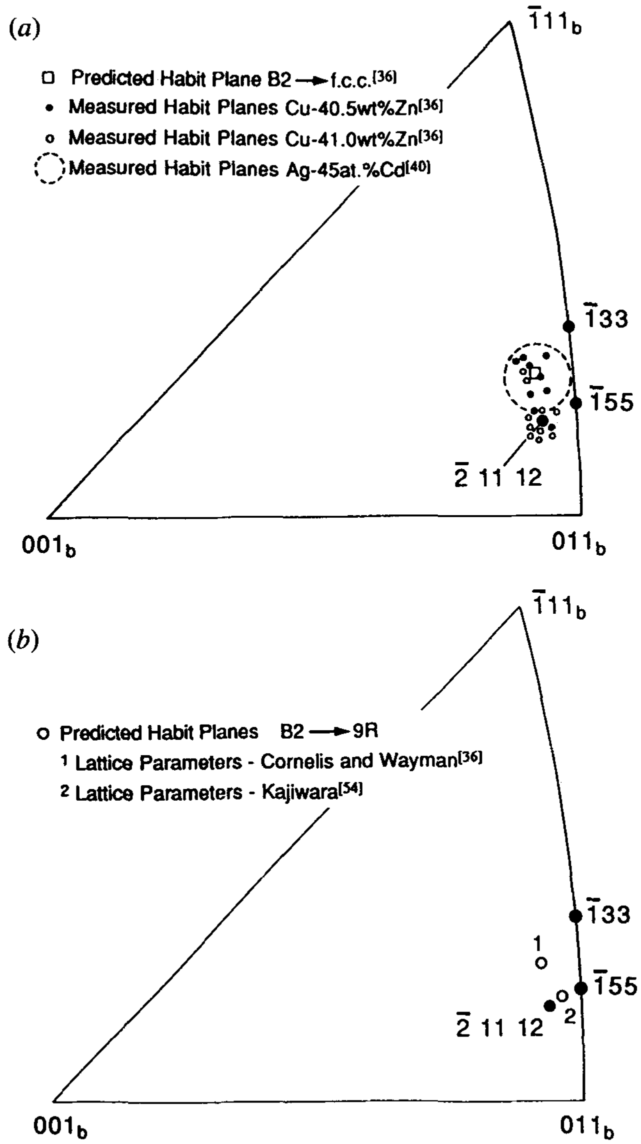

Fig. 10 — Stereographic projections showing (*a*) measured habit plane normals for α_l plates formed in two Cu-Zn alloys[36] and a Ag-Cd alloy[40] and (*b*) theoretical predictions of the habit plane for the *B*2 to 9*R* transformation.

the parent bcc (b) lattice in stereographic projection. The circle of radius 3.5 deg represents the scatter of two-thirds of individual measurements recorded for a Ag-45 at. pct Cd alloy,[40] while the individual measurements are reproduced for the Cu-Zn alloys. The habit plane is irrational and some 3.5 deg from $(\bar{1}44)_b$ or $(\bar{1}55)_b$; in the case of the Cu-41 wt pct Zn alloy, it is described[36] as being close to $(\bar{2},11,12)_b$. The large scatter in individual results reflects in part the limited accuracy of measurements made on what are very fine-scale plates, but it has also been suggested[36] that there is a significant variation in habit plane between the two Cu-Zn alloys due to a variation in lattice parameters. In both alloys, it is common for the α_l plates to form in chevron pairs, with the habit plane poles of the pair crystallographically equivalent and symmetrically distributed with respect to the nearest $\{011\}_b$ pole. Given the fine scale of the plates, complete measurements of the shape strain have not been made, but the surface tilts associated with plates formed at free surfaces have been reported to range up to 11.75 deg in the case of Cu-Zn alloys[36] and 12.0 ± 1.0 deg for the Ag-Cd alloy.[40]

Figure 11(a) shows an electron micrograph of an α_l plate formed during the early stages of transformation in a Ag-45 at. pct Cd alloy.[41] Given the limited scale of such plates, the orientation relationship between the β' and 9*R* α_l structures has commonly been determined approximately using conventional SAED patterns such as that of Figures 11(b) and (c), in which a $\langle 110\rangle_{9R}$ zone axis is approximately parallel to a $\langle 111\rangle_b$ zone of the parent phase and the close-packed planes of the α_l phase, $(009)_{9R}$, are parallel to the electron beam. The relationship that may be derived[36,38,40,41] from this and other zone axis patterns is irrational and is usually described approximately by the relationships between planes shown in Table III. The variant of the orientation relationship recorded in Table III corresponds to the variant of the habit plane shown in Figure 10.

The α_l plates have a substructure of parallel stacking faults distributed regularly along the length of each plate (Figure 11). For the variant of the habit plane shown in Figure 10 and the orientation relationship reported earlier, it has been established that the fault plane is $(111)_f$, derived from a $\{101\}_b$ plane of mirror symmetry in the parent bcc phase. With extended isothermal aging, the faulted substructure observed in freshly formed plates is annealed from the plates, and this recovery is accompanied by a transition in structure from the metastable 9*R* to the equilibrium 3*R* packing of close-packed planes (α).[36,40,41] Local growth of the plates proceeds behind incoherent, faceted interfaces, with interface facets bearing no apparent relationship to the original habit plane.

B. *Application of the Theory*

The formal theory has been applied to the formation of α_l plates in Cu-Zn[36] and Ag-Cd[40] alloys assuming a product structure that is fcc (3*R*) or fct ($c/a \sim 0.98$). The correspondence between bcc and fct lattices, identified as compatible with the observed orientation relationship, is equivalent to the reverse of the familiar Bain correspondence observed in association with the fcc to bct transformation in ferrous martensites.[4,42] When a strict correspondence of atom positions is preserved during transformation, this correspondence requires that the product phase remain ordered and acquire the fct CuAu I structure ($L1_0$). If the stacking faults within the plates are taken as evidence of the LIS, then the fault plane consistent with the variant of the correspondence is $(111)_f$ and, of the three $\langle 112\rangle_f$ directions in this plane, only a shear in the $[11\bar{2}]_f$ direction preserves the ordered arrangement in the product structure.[36] It has thus been assumed that the LIS comprises a shear on the system $(111)_f[11\bar{2}]_f$, which corresponds to a $\{110\}_b\langle 110\rangle_b$ shear system in the bcc matrix phase.

Based on these assumptions, the predictions of the theory for the components of the shape strain and the orientation relationship have been shown to be in good general agreement with experimental observations. The magnitude of the LIS predicted is in the range of 0.234[36] to 0.238[40] (corresponding to shear angles of

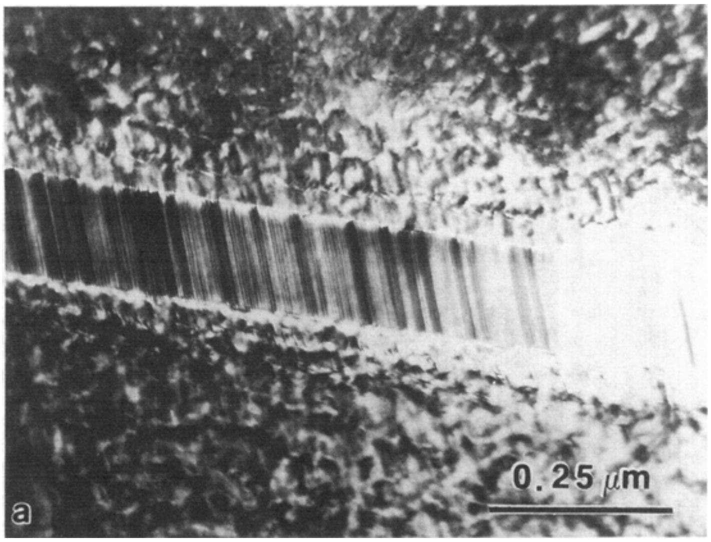

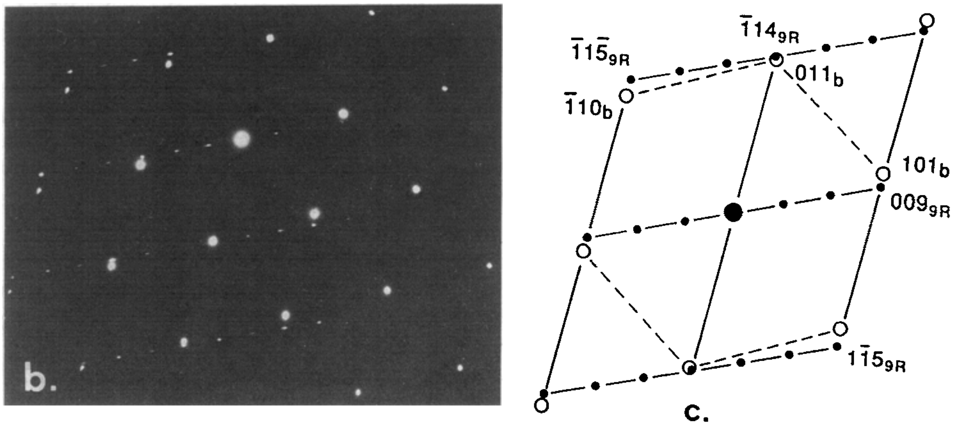

Fig. 11—(*a*) Transmission electron micrograph of α_1 plate in Ag-45 at. pct Cd alloy aged 30 s at 240 °C; (*b*) corresponding SAED pattern indicating approximately parallel $[\bar{1}\bar{1}1]_b$ and $[\bar{1}\bar{1}0]_{9R}$ zone axes from matrix and precipitate phases, respectively; and (*c*) schematic indexing of (b).

13.18 to 13.56 deg) and is almost exactly equivalent to the shear of $(a/6)[11\bar{2}]_f$ on every third $(111)_f$ plane that is required to generate the 9*R* stacking from a regular 3*R* fcc structure (*i.e.*, a shear of 13.26 deg). However, given the periodicity of these displacements, it is not expected that the modulation in stacking characteristic of the 9*R* structure will be resolvable using conventional electron imaging techniques. The stacking faults that are readily resolved within the α_1 plates are much more widely spaced and less regularly distributed than those that would be required to produce the 9*R* structure from conventional fcc, and this approach to application of the theory does not yield an obvious explanation of these faults. To account for faulting on the scale observed requires a more rigorous application of the theory, assuming that the product structure is 9*R* rather than fcc(t). Indeed, there is evidence to suggest that the 9*R* structure might properly be treated as a structure intermediate between the *B*2 parent and the equilibrium 3*R* phase, and that it is inappropriate to interpret the transformation as *B*2 to fcc 3*R*.

As indicated schematically in Figure 12, the 9*R* structure may be described by a unit cell that is orthorhombic if the structure is ideally close-packed and monoclinic (with a monoclinic β angle close to 90 deg) if there is a significant deviation from close packing normal to the close-packed planes.[54] The correspondence between parent bcc and product monoclinic (m) 9*R* lattices is such that the vectors $[10\bar{1}]_b$, $[010]_b$, and $[504]_b$ become the base vectors $[100]_m$, $[010]_m$, and $[001]_m$, respectively, in the product lattice. The LIS system corresponding to $(101)[10\bar{1}]_{bcc}$ and to $(111)[11\bar{2}]_{fct}$ is $(001)[100]_{9R}$. Reliable measurements of the lattice parameters of the isothermal 9*R* product are not readily available, but a range of parameters has been reported for the 9*R* martensite in Cu-Zn and Cu-Al systems.[36,54] Table IV presents a set of solutions to the crystallographic theory based on the above lattice correspondence and LIS, and a monoclinic 9*R* structure with a representative set of lattice parameters.

For the lattice parameters used in the compilation of Table IV, the predicted habit plane for low shear solution 1A, shown in Figure 10(b), is irrational. It lies within approximately 1.5 deg of $(\bar{1}55)_b$ and 1 deg of $(\bar{2},11,12)_b$ and is thus in good agreement with experimental observations of the habit plane for the Cu-41Zn

Table III. Comparison of Measured and Predicted Orientation Relationships for the *B*2 to 9*R* Transformation in Cu-Zn and Ag-Cd Alloys

	Measured Angles (deg)			Predicted Angles* (deg)
	Cu-Zn[36]	Ag-Cd[40]	Ag-Cd[41]	
$[110]_{9R} \wedge [\bar{1}\bar{1}1]_b$	~0.0	0.7 ± 0.2	<1.0	0.54
$(009)_{9R} \wedge (101)_b$	5.5	4.3 ± 0.4	5.0 ± 1.0	4.10
$(\bar{1}14)_{9R} \wedge (011)_b$	0.0 ± 0.5	—	<0.5	0.24
$(\bar{1}1\bar{5})_{9R} \wedge (\bar{1}10)_b$	5.5 ± 0.5	—	4.0 ± 1.0	3.90

*Calculated using the lattice parameters shown in Table IV.

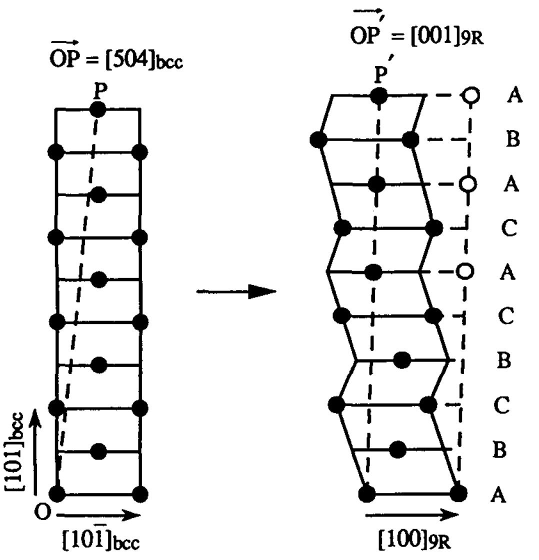

Out of plane normal = $[0\bar{1}0]_{bcc}$ Out of plane normal = $[0\bar{1}0]_{9R}$

Fig. 12—Schematic representation of the structural transformation from *B*2 to 9*R*, indicating the lattice correspondence that is sustained.

alloy reproduced in Figure 10(a). The habit plane predicted for the bcc to 9*R* transformation using the parameters of Cornelis and Wayman[36,53] (Figure 10(b)) is similar to that reported by those authors for the bcc to fct transformation and is in good agreement with experimental observations for the Cu-40.5Zn alloy in Figure 10(a). It is clear that the position of the predicted habit plane normal is sensitive to small variations in lattice parameters and that the theory is capable of accounting for the variation in the observed habit planes in Cu-Zn and Ag-Cd alloys, allowing for reasonable variations in the lattice parameters of the parent and product phases with varying alloy compositions.

For the habit plane variant shown in Figure 10 (low shear solution 1A), the predicted shape strain direction is also irrational, and approximately 8 deg from $[01\bar{1}]_b$ and within 2 deg of being parallel to the habit plane. The predicted shape strain displacement (m) is approximately 0.203. If an α_1 plate were to form at a free surface in such a way that the shear component of displacement was parallel to the surface normal, then the shape strain displacement would lead to a maximum surface tilt of ~11.48 deg. The predicted shape strain is thus capable of accounting well for observed surface tilts, which range up to a maximum of 11.75 deg and

Table IV. Predictions of the Crystallographic Theory for the *B*2 (b) to Monoclinic (m) 9*R* Transformation Associated with the Formation of α_1 Plates

Lattice Parameters: Parent bcc: $a_b = 0.2930$ nm
Product monoclinic 9*R*: $a_m = 0.4439$ nm, $b_m = 0.2638$ nm, $c_m = 1.921$ nm, $\beta_m = 89$ deg
Lattice Invariant Shear: $(101)[10\bar{1}]_{bcc} \rightarrow (111)[11\bar{2}]_{fct}$ and $(001)[100]_{9R}$
Lattice Correspondence: $[10\bar{1}]_b \rightarrow [100]_{9R}$ $[100]_b \rightarrow 1/9\ [401]_{9R}$
$[010]_b \rightarrow [010]_{9R}$ $[010]_b \rightarrow [010]_{9R}$
$[504]_b \rightarrow [001]_{9R}$ $[001]_b \rightarrow 1/9[\bar{5}01]_{9R}$

Solution	g	Habit Plane Normal Direction Cosines	Shape Strain Direction Cosines	m	Orientation Relationship: Direction Cosines of Product Axes		
					a_m	b_m	c_m
1A	0.00571	0.1325, −0.6821, −0.7192	0.1193, 0.7527, −0.6475	0.2031	0.67368	−0.01836	0.75044
					0.08596	0.99485	−0.05215
					−0.73400	0.09965	0.65888
1B	0.00571	0.1325, 0.6821, −0.7192	0.1193, −0.7527, −0.6475	0.2031	0.67368	0.01836	0.75044
					−0.08596	0.99485	0.05215
					−0.73400	−0.09965	0.65888
2A	0.18294	0.7192, −0.6821, −0.1325	0.6475, 0.7527, −0.1193	0.2031	0.73400	−0.09965	0.68450
					0.08596	0.99485	0.05515
					−0.67368	0.01836	0.72692
2B	0.18294	0.7192, 0.6821, −0.1325	0.6475, −0.7527, −0.1193	0.2031	0.73400	0.09965	0.68450
					−0.08596	0.99485	−0.05515
					−0.67368	−0.01836	0.72692

12.0 ± 1.0 deg in Cu-Zn[36] and Ag-Cd[40] alloys, respectively. Measured and predicted orientation relationships are also in excellent agreement, as shown in Table III. The angles between the pairs of planes and directions identified conveniently from SAED patterns agree to within experimental error on the measurements, and it is possible, on closer analysis, to confirm that the sense of the rotations predicted agrees with those observed.

An interesting feature of the solutions to the theory for the $B2$ to $9R$ transformation presented in Table IV is that they show that, for the lattice parameters employed, the total lattice strain may approximate to an invariant plane strain and that the magnitude of the LIS required is small ($g \sim 0.006$). Indeed, as indicated in Figure 13, the predicted magnitude of LIS may be reduced to zero with small changes in lattice parameters. Figure 13 shows the predicted variation in g with systematic variation in the parameters of the product monoclinic $9R$ phase about the commonly reported values, for a constant value of $a_b = 0.2930$ nm. For the low shear solutions, the magnitude of LIS is seen to be independent of b_m, but to vary significantly with a_m, c_m, and β_m and to approach zero at values of each of these parameters that are close to those used in the calculations for Table IV. For $g = 0$, the product phase would be expected to have a fault-free $9R$ structure and to be coherent with the matrix β' phase across the irrational habit plane. However, for lattice parameters leading to a finite value of g, the α_1 plates would be expected to have a substructure of coarsely spaced stacking faults, in qualitative agreement with common observations for α_1 plates in Cu-Zn and Ag-Cd alloys. The magnitude of g and thus the spacing of the stacking faults arising as the result of the LIS would be expected to vary with variation in lattice parameters. For the parameters employed by Cornelis and Wayman,[36,53] for example, the predicted magnitude of g rises to ~0.012 and the corresponding α_1 plates would be expected to contain a higher density of internal faulting arising from the LIS.

VI. DISCUSSION

As is the case for the martensitic fcc to hcp transformation, the structural change associated with the γ' precipitate plates in Al-Ag alloys may be considered to be accomplished by the passage of transformation dislocations across the broad faces of the plates.[48,49] Defining steps that are two close-packed planes in height normal to the habit plane, these transformation dislocations have a Burgers vector that is of the form $(a/6)\langle 11\bar{2}\rangle$ in the case of coherent transformation to an ideal hcp structure with zero volume change, but that must acquire a small additional component of magnitude ξ normal to the habit plane, *i.e.*, $(2a\xi/3)\langle 111\rangle$, for the γ' phase. For such transformations, formal application of the crystallographic theory, assuming the total lattice strain $\mathbf{S}_T$ to be an invariant plane strain on the $(111)_f$ habit plane with a displacement $m\mathbf{d}$ equivalent to the Burgers vector of the transformation dislocations, provides a complete description of the transformation crystallography.

For both the martensitic fcc to hcp transformation and the formation of γ' plates, there is strong experimental evidence to support the proposal that the fcc to hcp transition involves the lateral migration of steps across the otherwise coherent broad faces of the product phase, with the steps having the configuration of the transformation dislocations required by the theory. High-resolution electron microscope images,[22,23] recorded parallel to close-packed (*i.e.*, $\langle 110\rangle_f \| \langle 11\bar{2}0\rangle_h$) directions in the habit plane, reveal that the interface commonly contains steps normal to the habit plane that are invariably an even multiple of close-packed layers in height and that may be interpreted as an accumulation of $(a/6)\langle 11\bar{2}\rangle$ Shockley partial transformation dislocations on every second close-packed $(111)_f$ plane. Single transformation dislocations are observed, but it is more common for the observed steps to comprise multiple dislocations. Since the layer of atoms (1) immediately

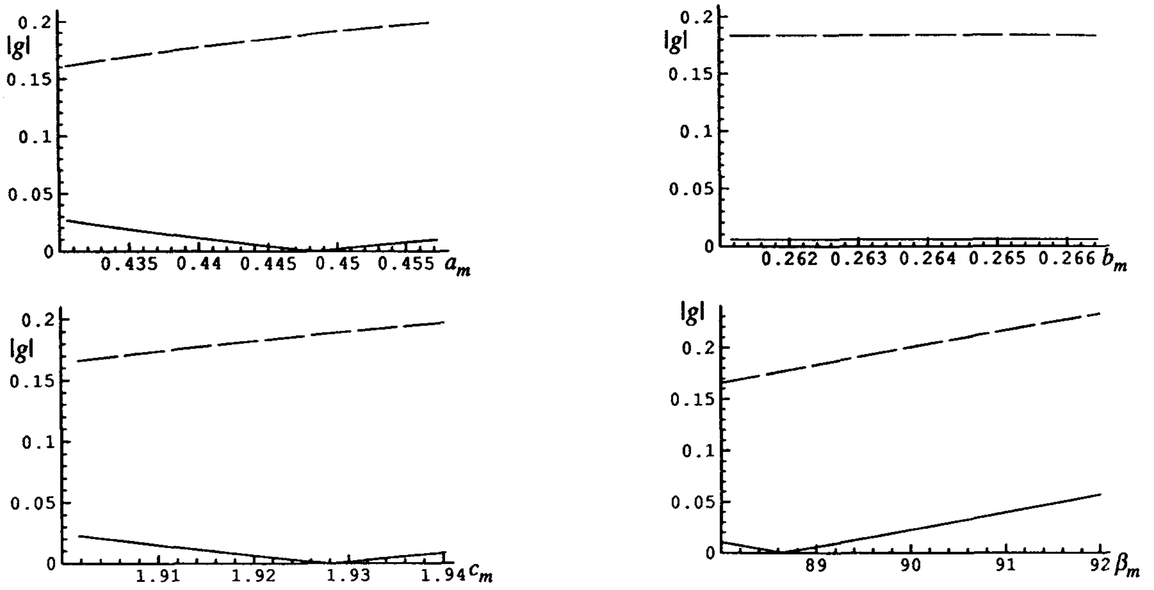

Fig. 13—Predicted variation in the magnitude (g) of the LIS with variation in each of the product lattice parameters a_m, b_m, c_m, and β_m for the $B2$ to $9R$ transformation. The lattice parameter of the parent phase a_b is assumed constant.

ahead of the interface in Figure 1(a) may be regarded as common to the fcc and hcp lattices, it has been suggested[23] that there may be some adjustment in composition in this layer ahead of the passage of a transformation dislocation. However, the completion of the structural transition requires the migration of a transformation dislocation over the next adjacent layer in the fcc phase and an adjustment in the composition that allows this plane of the precipitate to contain wholly Ag atoms. It is inferred that passage of the transformation dislocation involves atom by atom transfer between parent and product phases, with Ag atoms attaching themselves preferentially at kink sites along the Shockley partial transformation dislocations. The rate of migration may be controlled either by long-range transport of Ag atoms ahead of the migrating transformation dislocations or by the substitutional diffusion of Ag atoms across the kinks. Although there is a substantial compositional change associated with the transformation, the diffusion-controlled migration of the transformation dislocations in the manner described permits a coherent interface to be sustained and to migrate normal to the habit plane to sustain thickening of the plate and the maintenance of a correspondence of lattice sites.

In a given $\{111\}_f$ habit plane there are three equivalent $\langle 11\bar{2}\rangle_f$ twinning directions, and the passage of a transformation dislocation with a Burgers vector given by Eq. [2] in any one of these directions will generate the observed hcp structure. If the transformation involves migration of transformation dislocations in a single $\langle 11\bar{2}\rangle_f$ direction on alternate $(111)_f$ planes, then an appreciable shape change will accumulate over the transformed volume. When the component of displacement normal to the habit plane is zero, this shape change will be a simple shear, but if the normal component of displacement is finite, then the shape change will have the more general form of an invariant plane strain. If, alternatively, transformation dislocations are generated in all three $\langle 11\bar{2}\rangle_f$ directions and the transformed volume contains equal volume fractions of all three variants of the hcp structure, then the variants will be self-accommodating and the shear component of the net shape deformation over the transformed volume will be zero. Of course, it is possible to imagine situations between these two extremes,[49] but for transformation product forming within the bulk constraints of the parent phase it is to be expected that all three transformation variants will operate within a given product plate to minimize the shape deformation, which is consistent with direct experimental observations for bulk γ' plates in Al-Ag.[23] If, however, the transformation were to occur under the influence of an applied stress with a significant shear component, then an interaction that relaxed the potential of the stress field might be expected to favor the adoption of one preferred shear component of transformation and the development of a significant shape change. Similarly, for those plates nucleating at or in the immediate vicinity of a free surface, the relaxed matrix constraints may lead to preference for a single set of transformation dislocations and the accumulation of a finite shape deformation that approaches one-half the twinning shear in magnitude. Such is the explanation offered[55] for the observation of invariant plane-strain surface relief associated with at least some γ' precipitate plates at free surfaces in Al-Ag alloys.

The formation of the ordered orthorhombic phase AuCu II from disordered fcc parent phase also generates invariant plane-strain surface relief and conforms with predictions of the crystallographic theory.[25] Based on the assumptions that the lattice correspondence is identity and the LIS is a partial twinning shear on the system $(101)[\bar{1}01]$, the theory is capable of accounting consistently and accurately for the observed habit plane, surface relief, and orientation relationship. With appropriate choice of variants of the lattice correspondence, it is also capable of generating crystallographic variants of the habit plane normal and displacement direction that each cluster about common $\langle 110\rangle_f$ directions, and thus account for the growth of AuCu II plates in partially self-accommodating pairs or pyramidal groups. Moreover, recent measurements[52] have confirmed that the observed fine-scale twinning within AuCu II plates is on the appropriate twinning system required by the theory and that the relative fraction of the twin-related variants within a given plate is accurately consistent with the magnitude of the LIS required to ensure that the irrational habit plane is macroscopically invariant. It is thus strongly suggested that the twinned substructure of the plates is a direct manifestation of the LIS.

The AuCu II plates have a form and substructure similar to those of martensite plates in which the LIS involves twinning of the product structure, and the faceted interface between twinned product and single-crystal matrix that is evident in Figures 7 and 9 is typical of one of the two common models proposed for a semicoherent martensite interface.[48,49,50] In this model, the interface facets define areas of coherence between parent and product lattices, separated periodically in the product phase by twin boundaries. For a diffusionless, martensitic transformation, such an interface is considered to be glissile and capable of migration as an entity normal to the habit plane through homogeneous transformation of the coherent regions combined with extension of the twin boundaries to preserve an invariant habit plane. However, for an ordering transformation involving nearest-neighbor exchange of atoms, such as the formation of AuCu II plates, it is currently not clear that migration of such a semicoherent interface in the direction of its normal will sustain the coordinated atom displacements necessary to the maintenance of a correspondence of lattice sites.

To resolve this apparent difficulty, it has been proposed[29] that both lengthwise growth and thickening of AuCu II plates involve the generation and glide of transformation dislocations parallel to the habit plane. For a pyramidal group of four plates such as that illustrated schematically in Figure 4, it is suggested that the dislocations responsible for growth on the inner surfaces of the pyramid would be generated cooperatively at the common inner apex. The Burgers vectors $m\mathbf{d}$ of the dislocations on the four plates would be equal in magnitude and approximately parallel to the same $[110]_f$ direction. It is anticipated that the individual dislocation segments would form a continuous loop around the inner surface of the pyramid and that cooperative glide across the broad inner surfaces of the plates would allow the four plates to grow at the same rate, with the inner apex moving parallel to the $[0\bar{1}1]_f$ axis of the pyramid. The inner surfaces of the pyramid would likely contain steps corresponding to single or multiple transformation dislocations and, if growth were largely confined to the inner surfaces of the pyramid, the plates would become tapered in section, with the inner surfaces and their junction lines deviating significantly from the corresponding habit planes and habit plane intersections.

The form and crystallography of the proposed transformation dislocations have not been addressed in detail, and the compatibility of the transformation dislocations, which generate the observed shape deformation, with the internal twinning, which must occur within the lattice created by the shape strain and, on this interpretation, constitutes evidence of the complementary strain of the original Bowles-Mackenzie formulation of the crystallographic theory,[2] requires further examination. However, it has been demonstrated that the model of the growth mechanism based on such transformation dislocations is consistent with the morphology of AuCu II plates and with measurements of both the lengthening and thickening kinetics of plate growth. The migration of transformation dislocations within the habit plane also provides a plausible mechanism by which a correspondence of lattice sites may be sustained in the face of the atomic interchange necessary to accomplish the ordering reaction. The atomic displacements are restricted to coordinated atom transfer at single dislocation steps, and it is suggested that the dislocations will migrate at a rate determined by the rate of ordering of atoms at the steps. It is in the nature of these steps and the mechanism of atom transfer across the steps that the proposed mechanism differs significantly from earlier models,[27,28] in which separate mechanisms were proposed for lengthening and thickening of plates and in which plate thickening was proposed to involve the migration of disordered ledges across the habit plane interface. It remains difficult to reconcile the maintenance of a lattice correspondence and the resulting generation of an invariant plane-strain shape change with a mechanism in which random atom transfer occurs across disordered ledges in the interface. Unlike the γ' precipitate plates in Al-Ag alloys, there have to date been no detailed studies of the interface structure in AuCu II plates, and there thus remains little direct evidence on which to assess the proposed transformation mechanisms.

While there is no composition change associated with the growth of ordered AuCu II plates, the question of whether there is a change in composition accompanying the initial formation of α_1 plates in Cu-Zn(-X) and Ag-Cd alloys is central to the present discussion and the answer remains controversial.[41,56–62] The bulk of current evidence strongly suggests that there is a significant difference in composition between the α_1 plates and β' matrix at the earliest stages of transformation for which measurements can presently be made. There is also evidence from some studies[37,38,41] that the order present in the matrix β' phase is not necessarily preserved in the formation of the 9*R* plates, confirming the existence of significant atomic interchange accompanying initial growth. In the Ag-Cd system it has been confirmed[41] that the α_1 plates have a disordered 9*R* structure, in conjunction with a composition approaching that of the equilibrium α phase, well before any evidence of the 9*R* to 3*R* structural transition that accompanies prolonged isothermal aging. It is thus difficult to sustain an argument that initial growth is diffusionless with a subsequent adjustment in composition, for it would require this adjustment in composition to preserve the 9*R* structure, only to have it subsequently transform to equilibrium 3*R*. Even if, as has been suggested,[41,60] the α_1 plates lengthen in a displacive (diffusionless) manner and then thicken at a rate controlled by substitutional volume diffusion, there is no evidence to suggest that the plates are composite in structure and the lateral growth must thus occur in such a way that the 9*R* structure, lattice correspondence, and shape change are sustained during diffusional growth.

Formation of the α_1 plates produces a shape change compatible with an invariant plane strain, and the crystallographic theory again provides an excellent basis for accounting for the observed crystallographic features of the transformation. Although initial applications[36,40] of the theory, which assumed for convenience the product structure to be fcc(t), produced predictions in general agreement with experimental observations, the present analysis suggests that this interpretation may be in part misleading. In the early analyses, the magnitude of the LIS on the observed slip system required to preserve an invariant habit plane was found to be approximately equivalent to the shear of $(a/6)[11\bar{2}]$ on every third (111) plane that would generate 9*R* stacking of the close-packed planes of a 3*R* fcc structure. This approach thus has the potential to create the impression that the 9*R* structure of the α_1 plates is a consequence of the LIS component of the shape strain, rather than the preferred product structure in the initial stages of decomposition of supersaturated β' phase. It also fails to provide a sound basis for accounting for the substructure of stacking faults in α_1 plates, for those faults detectable are much more widely spaced than every third {111} plane.

If a comparison is made of the principal distortions (η_i) of the homogeneous lattice deformations **B** for the *B*2 to 9*R* and *B*2 to fcc(t) transformations, then, as shown in Table V, those associated with the *B*2 to 9*R* transition are much closer to unity than those for the transformation to the fcc(t) structure. This implies that the lattice distortion associated with formation of the 9*R* structure is significantly less than that required to form the fcc structure and suggests that it is more appropriate to regard the 9*R* structure as a preferred metastable phase, intermediate between the parent *B*2 β' and equilibrium product α. In support of this interpretation, it is to be noted that the magnitude (g) of the LIS required for the *B*2 to 9*R* transition approaches zero for small variations in lattice parameters from observed values. For $g = 0$, the α_1 plates would be expected to be fully coherent with the parent phase and grow fault-free. This may account for the recent, and yet to be confirmed, observation of coherent α_1 plates free of faulted substructure in the very early stages of transformation in a Cu-Zn alloy.[39] It has been suggested[39] that such plates represent the initial growth stage for α_1 plates and that

Table V. Comparison of the Principal Distortions η_i of the Homogeneous Lattice Strain B for the $B2$ to fcc(t) and $B2$ to $9R$ Transformations in Cu-Based Alloys

Transformation	η_1	η_2	η_3
$B2 \rightarrow$ fcc[36]	0.891894	0.891894	1.26133
*$B2 \rightarrow 9R$[54]	0.900341	0.997322	1.10645
**$B2 \rightarrow 9R$[36]	0.891891	0.994588	1.13109

*Calculated using the lattice parameters of Kajiwara[54] (Table IV).
**Calculated using $9R$ lattice parameters equivalent to those of Cornelis and Wayman.[36]

the plates subsequently acquire the faulted substructure in a second stage of growth, during which they lose coherency with the matrix. In formal terms, the crystallographic theory allows for the magnitude of the LIS to become finite, with small local variations in the lattice parameters at the transformation interface, perhaps as a result of local changes in composition. The theory thus allows for the development of a faulted substructure, although the mechanism by which faults apparently propagate through the existing volume of plate established during the initial coherent growth stage perhaps needs further attention. Irrespective of the outcome of such analysis, it is to be emphasized that, for the $B2$ to $9R$ transition and the available lattice parameters, the theory requires a small finite value of g and thus a substructure of relatively widely spaced stacking faults that is qualitatively consistent with observations.

Following a recent study of the structure of the broad faces of α_1 plates in a Cu-Zn alloy, it was reported that the plates develop growth ledges during the second stage of growth and suggested that growth proceeds *via* diffusion-controlled ledge wise thickening.[39,63] The observation of an invariant plane-strain shape change and the well-established applicability of the crystallographic theory imply that this growth should proceed in such a way that a correspondence of lattice sites is preserved. It thus seems likely that the growth ledges responsible for thickening should have the form of transformation dislocations gliding across the broad faces of the plates at a rate that is diffusion controlled. It is possible that a correspondence of sites may be maintained if there is a coordinated atom by atom transfer from parent to product phase at individual dislocation steps in the interface, but again unlikely that this will be so if the risers of the growth ledges are disordered or incoherent. The form and crystallography of any such ledges or transformation dislocations on the broad faces of α_1 plates remain unresolved in detail, and it would seem that prospects for progress in resolving details of the mechanism of the transformation rest with further detailed high-resolution studies of the interface and, as in the case of AuCu II plates, analysis of the compatibility of potential transformation dislocations with those responsible for the lattice invariant shear.

VII. SUMMARY

1. The transformation products associated with

(a) precipitation of hcp Ag_2Al (γ') plates in Al-Ag alloys;
(b) formation of ordered orthorhombic AuCu II plates in equiatomic Au-Cu; and
(c) formation of $9R$ α_1 plates in ordered $B2$ Cu-Zn(-X) and Ag-Cd alloys

produce relief at a free surface consistent with an invariant plane-strain change. The transformations are thus properly described as displacive.

2. The observed shape change implies that a lattice correspondence is maintained between parent and product phases. The existence of such a lattice correspondence is fundamental to justifying the application of the theory of martensite crystallography to this class of transformations.
3. The theory of martensite crystallography may be applied successfully to account for the crystallographic features of each of these transformations. The agreement between experimental observations and theoretical predictions is exceptionally good in all cases.
4. Although it has been common to assume that atomic interchange or a compositional change involving long-range substitutional diffusion is incompatible with the maintenance of a lattice correspondence, the formal crystallographic theory does not necessarily require a correspondence of atom positions and thus does not preclude interchange of atom positions or a change in composition. Successful application of the theory does, however, imply a transformation mechanism that is compatible with the maintenance of a correspondence of lattice sites.
5. It seems likely that the mechanism of transformations in this group involves the migration of transformation dislocations in the planar interface between parent and product, and coordinated atom by atom transfer across the interface associated with motion of the corresponding dislocation steps in the interface. The rate of migration of the transformation dislocations is controlled by the rate at which the required atoms assemble ahead of the migrating dislocation steps. The migration of the transformation dislocations produces the displacements that generate the surface relief.

REFERENCES

1. M.S. Wechsler, D.S. Lieberman, and T.A. Read: *Trans. AIME*, 1953, vol. 194, p. 1503.
2. J.S. Bowles and J.K. Mackenzie: *Acta Metall.*, 1954, vol. 2, pp. 129, 138, and 224.
3. A.F. Acton, M. Bevis, A.G. Crocker, and N.D.H. Ross: *Proc. R. Soc. (London) A*, 1970, vol. 320, p. 101.
4. C.M. Wayman: *Introduction to the Crystallography of Martensitic Transformations*, Macmillan, New York, NY, 1964.

5. J.W. Christian: *The Theory of Transformations in Metals and Alloys*, Pergamon Press, Oxford, 1975.
6. Z. Nishiyama: *Martensitic Transformation*, Academic Press, New York, NY, 1978.
7. B.C. Muddle and G.R. Hugo: *Proc. 7th Int. Conf. Martensitic Transformations (ICOMAT '92)*, Monterey, CA, 1992, in press.
8. J.D. Watson and P.G. McDougall: *Acta Metall.*, 1973, vol. 21, p. 961.
9. J.S. Bowles and N.F. Kennon: *J. Aust. Inst. Met.*, 1960, vol. 5, p. 106.
10. G.R. Srinivasan and C.M. Wayman: *Acta Metall.*, 1968, vol. 16, p. 621.
11. S. Hoekstra: *Acta Metall.*, 1980, vol. 28, p. 507.
12. B.P.J. Sandvik: *Metall. Trans. A*, 1982, vol. 13A, p. 777.
13. J.S. Bowles, B.C. Muddle, and C.M. Wayman: *Acta Metall.*, 1977, vol. 25, p. 513.
14. M.P. Cassidy, B.C. Muddle, T.E. Scott, C.M. Wayman, and J.S. Bowles: *Acta Metall.*, 1977, vol. 25, p. 829.
15. U. Dahmen, P. Ferguson, and K.H. Westmacott: *Acta Metall.*, 1987, vol. 35, p. 1037.
16. J. Van Landuyt and C.M. Wayman: *Acta Metall.*, 1968, vol. 16, p. 803.
17. C.M. Wayman and J. Van Landuyt: *Acta Metall.*, 1968, vol. 16, p. 815.
18. J.A. Hren and G. Thomas: *Trans. Met. Soc. AIME*, 1963, vol. 227, p. 308.
19. C. Laird and H.I. Aaronson: *Acta Metall.*, 1967, vol. 15, p. 73.
20. C. Laird and H.I. Aaronson: *Acta Metall.*, 1969, vol. 17, p. 505.
21. Y.C. Liu and H.I. Aaronson: *Acta Metall.*, 1970, vol. 18, p. 845.
22. J.M. Howe, H.I. Aaronson, and R. Gronsky: *Acta Metall.*, 1985, vol. 33, pp. 639 and 649.
23. J.M. Howe, U. Dahmen, and R. Gronsky: *Phil. Mag.*, 1987, vol. 56, p. 31.
24. J.S. Bowles and A.S. Malin: *J. Aust. Inst. Met.*, 1960, vol. 5, p. 131.
25. R. Smith and J.S. Bowles: *Acta Metall.*, 1960, vol. 8, p. 405.
26. A.M. Hunt and D.W. Pashley: *J. Aust. Inst. Met.*, 1963, vol. 8, p. 61.
27. A.J. Pedraza and J. Kittl: *Acta Metall.*, 1976, vol. 24, p. 835.
28. H.I. Aaronson and K.R. Kinsman: *Acta Metall.*, 1977, vol. 25, p. 367.
29. J.S. Bowles and C.M. Wayman: *Acta Metall.*, 1979, vol. 27, p. 833.
30. G. Van Tendeloo, S. Amelinckx, S.J. Jeng, and C.M. Wayman: *J. Mater. Sci.*, 1986, vol. 21, p. 4395.
31. R.D. Garwood: *J. Inst. Met.*, 1954–55, vol. 83, p. 64.
32. R.D. Garwood: *Iron Steel Inst. Spec. Rep.*, No. 93, 1965, p. 90.
33. P.E.J. Flewitt and J.M. Towner: *Acta Metall.*, 1966, vol. 14, p. 1013.
34. E. Hornbogen and H. Warlimont: *Acta Metall.*, 1967, vol. 15, p. 943.
35. P.E.J. Flewitt and J.M. Towner: *J. Inst. Met.*, 1967, vol. 95, p. 273.
36. I. Cornelis and C.M. Wayman: *Acta Metall.*, 1974, vol. 22, p. 301.
37. M.-H. Wu and C.M. Wayman: *Proc. Int. Conf. Martensitic Transformations*, Japan Institute of Metals, Sendai, Japan, 1986, p. 619.
38. M.-H. Wu, J. Perkins, and C.M. Wayman: *Acta Metall.*, 1989, vol. 37, p. 1821.
39. K. Chattopadhyay and H.I. Aaronson: *Acta Metall.*, 1986, vol. 34, p. 695.
40. M.M. Kostic and E.B. Hawbolt: *Metall. Trans. A*, 1979, vol. 10A, p. 165.
41. M.-H. Wu, B.C. Muddle, and C.M. Wayman: *Acta Metall.*, 1988, vol. 36, p. 2095.
42. J.S. Bowles and C.M. Wayman: *Metall. Trans.*, 1972, vol. 3, p. 1113.
43. J.W. Christian: *Proc. R. Soc. (London) A*, 1951, vol. 206, p. 51.
44. P. Gaunt and J.W. Christian: *Acta Metall.*, 1959, vol. 7, p. 529.
45. S. Mahajan, M.L. Green and D. Brasen: *Metall. Trans. A*, 1977, vol. 8A, p. 283.
46. C. Hayzelden, K. Chattopadhyay, J.C. Barry, and B. Cantor: *Phil. Mag.*, 1991, vol. A63, p. 461.
47. J.W. Brooks, M.H. Loretto, and R.E. Smallman: *Acta Metall.*, 1979, vol. 27, p. 1839.
48. J.W. Christian: in *Interfaces Conf.*, R.C. Gifkins, ed., Butterworth's, London, 1969, p. 159.
49. J.W. Christian: in *Martensite*, G.B. Olson and W.S. Owen, eds., ASM International Materials Park, OH, 1992, p. 103.
50. J.W. Christian and K.M. Knowles: in *Proc. Int. Conf. Solid-Solid Phase Transformations*, H.I. Aaronson, D.E. Laughlin, R.F. Sekerka, and C.M. Wayman, eds., TMS-AIME, Warrendale, PA, 1982, p. 1185.
51. J.W. Christian: *Decomposition of Austenite by Diffusional Processes*, Interscience, New York, NY, 1962, p. 371.
52. J.F. Nie and B.C. Muddle, Monash University, Clayton, Victoria, Australia, unpublished research, 1993.
53. I. Cornelis and C.M. Wayman: *Acta Metall.*, 1974, vol. 22, p. 291.
54. S. Kajiwara: *Trans. Jpn. Inst. Met.*, 1976, vol. 17, p. 435; 1976, vol. 17, p. 448.
55. U. Dahmen: *Scripta Metall.*, 1987, vol. 21, p. 1029.
56. I. Cornelis and C.M. Wayman: *Scripta Metall.*, 1973, vol. 7, p. 579.
57. G.W. Lorimer, G. Cliff, H.I. Aaronson, and K.R. Kinsman: *Scripta Metall.*, 1975, vol. 9, p. 271.
58. M.M. Kostic and E.B. Hawbolt: *Scripta Metall.*, 1975, vol. 9, p. 1173.
59. G.W. Lorimer, G. Cliff, H.I. Aaronson, and K.R. Kinsman: *Scripta Metall.*, 1975, vol. 9, p. 1175.
60. P. Doig and P.E.J. Flewitt: *Met. Sci.*, 1983, vol. 17, p. 601.
61. B.C. Muddle and H.L. Fraser: in *Proc. Int. Conf. Solid-Solid Phase Transformations*, H.I. Aaronson, D.E. Laughlin, R.F. Sekerka, and C.M. Wayman, eds., TMS-AIME, Warrendale, PA, 1983, p. 987.
62. Y. Nakata, T. Tadaki, and K. Shimizu: *Mater. Trans. JIM*, 1989, vol. 30, p. 107.
63. H.I. Aaronson, T. Furuhara, J.M. Rigsbee, W.T. Reynolds, Jr., and J.M. Howe: *Metall. Trans. A*, 1990, vol. 21A, p. 2369.